

Massive Neutrino Decays.

Pham Xuan Yem ¹

*Laboratoire de Physique Théorique et Hautes Energies, Paris
CNRS, Université P. et M. Curie, Université D. Diderot*

Abstract-

Lecture given at the Vth Viet Nam School of Physics, Hanoi 28 December 1998 - 9 January 1999. Neutrino physics is used as an illustrative example for an elementary introduction to the computational method of Feynman loop-diagrams and decay rates.

If the neutrinos are as massive as recently reported by the Super-Kamiokande results, the heaviest neutrino ν_H would not be stable. Although chargeless, it could decay – by quantum loop effect – into a lighter neutrino ν_L by emitting a photon: $\nu_H \rightarrow \nu_L + \gamma$. If kinematically possible, the $\nu_H \rightarrow \nu_L + e^+ + e^-$ mode could occur at the tree diagram level and furthermore get enhanced, at one-loop radiative corrections, by a large logarithm of the electron mass acting as an infrared cutoff.

¹Postal address: LPTHE, Tour 16, 1^{ère} Etage, 4 Place Jussieu, F-75252 Paris CEDEX 05, France.

Electronic address : pham@lpthe.jussieu.fr

Evidence for the transmutation between the two neutrino species $\nu_\mu \leftrightarrow \nu_\tau$ is recently reported by the Super-Kamiokande collaboration⁽¹⁾. As a consequence, neutrinos could have nondegenerate tiny masses, and mixing among different lepton families would occur, similarly to the Cabibbo–Kobayashi–Maskawa (CKM) flavor mixing in the quark sector. Let us start by assuming that the neutrino flavored states ν_e , ν_μ and ν_τ are linear combinations of the three neutrino mass eigenstates ν_1 , ν_2 and ν_3 of nonzero and nondegenerate masses m_1 , m_2 and m_3 respectively. Thus

$$\begin{pmatrix} \nu_e \\ \nu_\mu \\ \nu_\tau \end{pmatrix} = \begin{pmatrix} U_{e1} & U_{e2} & U_{e3} \\ U_{\mu 1} & U_{\mu 2} & U_{\mu 3} \\ U_{\tau 1} & U_{\tau 2} & U_{\tau 3} \end{pmatrix} \begin{pmatrix} \nu_1 \\ \nu_2 \\ \nu_3 \end{pmatrix} \equiv \mathcal{U}_{\text{lep}} \begin{pmatrix} \nu_1 \\ \nu_2 \\ \nu_3 \end{pmatrix}, \quad (1)$$

where the 3×3 matrix \mathcal{U}_{lep} is unitary. Neutrino oscillation measurements give constraints usually plotted in the $(\sin 2\theta_{ij}, \Delta m_{ij}^2 = |m_i^2 - m_j^2|)$ plane, where θ_{ij} is one of the three Euler angles of the rotation matrix \mathcal{U}_{lep} . The effective weak interactions of leptons can now be written as

$$\mathcal{L}_{\text{eff}} = \frac{G_F}{\sqrt{2}} L_\lambda^\dagger L_\lambda,$$

where the charged current L_λ is

$$L_\lambda = \sum_\ell \sum_{i=1}^3 U_{\ell i} \bar{\nu}_i \gamma_\lambda (1 - \gamma_5) \ell.$$

Here ℓ stands for e^- , μ^- , τ^- and ν_i (with $i = 1, 2, 3$) are the three neutrino mass eigenstates. Unitarity of \mathcal{U}_{lep} implies that for any fixed ℓ , one has $\sum_i |U_{\ell i}|^2 = 1$, or $\sum_i U_{\ell i} U_{\ell' i}^* = \delta_{\ell\ell'}$ and $\sum_\ell U_{\ell i} U_{\ell j}^* = \delta_{ij}$. This current L_λ tells us for instance that the neutrino ν_μ operationally defined to be the invisible particle missing in the decay $\pi^+ \rightarrow \mu^+ + \nu_\mu$ is initially a superposition of ν_1 , ν_2 and ν_3 , in the same way as the K^0 meson produced by strong interaction is initially a superposition of the mass eigenstates K_L^0 and K_S^0 with masses $m_L \neq m_S$. The nondegenerate masses give rise to the oscillation phenomena in both neutral K mesons and neutrinos.

Moreover, although the neutrinos are chargeless, a heavy neutrino ν_H could decay into a lighter neutrino ν_L by emitting a photon; this decay is entirely due to quantum loop effects. If kinematically possible, i.e. if the $\nu_H - \nu_L$ mass difference is larger than twice the electron mass (≈ 1 MeV), then the mode $\nu_H \rightarrow \nu_L + e^+ + e^-$ largely dominates, because it is governed by a tree diagram and enhanced by radiative corrections, as we will see.

1- One-loop effective $\nu_i\text{-}\nu_j\text{-}\gamma$ vertex Γ^μ

In gauge theories with spontaneous symmetry breaking, by the power counting arguments, renormalizability of electroweak interactions is not manifest in the unitary U gauge^{2,3} where only physical gauge bosons W, Z are involved. This is because of the bad high-energy behavior of massive W, Z propagators [$D(k) \rightarrow 1/M_{W,Z}^2$ for $k \rightarrow \infty$]. With the U gauge, except for lowest orders (tree diagrams), it is practically impossible to perform higher order calculations, because the k integrations in loop diagrams cause an avalanche of uncontrollable quadratic divergences.

On the other hand, the renormalizable gauge^{2,3} (conventionally called R_ξ) is particularly convenient for loop calculations. As shown by 't Hooft, the key is to choose a gauge parameter ξ with which the gauge boson propagator has a mild high-energy behavior ($D(k) \rightarrow 1/k^2$ for $k \rightarrow \infty$), at the expense of introducing fictitious particles, the "would be" Goldstone bosons Φ (those absorbed by the weak gauge bosons to render them massive by the Higgs mechanism). Feynman rules for the W and Φ propagators, as well as for some vertices in the R_ξ gauge are given in the appendix, from which we compute loop amplitudes.

In R_ξ at one loop level, six Feynman diagrams contribute to the process $\nu_H(P) \rightarrow \nu_L(p) + \gamma(q)$, where the photon can be real ($q^2 = 0$) or virtual ($q^2 \neq 0$); the latter is necessary when we consider the radiative corrections to the $\nu_H \rightarrow \nu_L + e^+ + e^-$ tree diagram. These six diagrams can be grouped into two sets: four in Figs. 1a–1d and two in Fig.2a–2b. Every diagram is gauge-dependent through a ξ parameter, however the ξ -dependences are canceled out separately for each group, i.e. the sum of the four diagrams in Fig.1 is ξ -independent; the same occurs for the sum of the two diagrams in Fig.2. Consequently, the final result is *gauge-independent*, as it should be for any physical process. In the U gauge corresponding to $\xi = \infty$, only two diagrams (Fig.1a and Fig.2a) contribute; the price to pay is the bad high-energy behavior of the W boson propagator which renders the loop integration particularly difficult.

• Let us explicitly compute, as an example, the simplest amplitude \mathcal{A}_{1b} associated with the diagram of Fig.1b in the general R_ξ gauge for which Feynman rules give

$$i \mathcal{A}_{1b} = (-ie) \left(\frac{ig}{2\sqrt{2}} \right)^2 \sum_{\ell} U_{L\ell} U_{H\ell}^* \bar{u}(p) \Gamma_{1b}^\mu(\ell) u(P) \varepsilon_\mu^*(q), \quad (2)$$

$$\Gamma_{1b}^\mu(\ell) = \int \frac{d^4k}{(2\pi)^4} \frac{[m(1-\gamma_5) - m_\ell(1+\gamma_5)][i(\not{k} + m_\ell)][M(1+\gamma_5) - m_\ell(1-\gamma_5)](P+p-2k)^\mu}{M_W^2 [(k-p)^2 - \xi M_W^2][(P-k)^2 - \xi M_W^2](k^2 - m_\ell^2)}, \quad (3)$$

where m and M are respectively the light ν_L and the heavy ν_H neutrino masses, m_ℓ ($\ell = 1, 2, 3$) stand for e^- , μ^- and τ^- masses, and $\varepsilon_\mu^*(q)$ denotes the photon polarization four-vector. $\Gamma_{1b}^\mu(\ell)$ is the contribution of Fig.1b to the effective neutrinos-photon vertex Γ^μ . To simplify the computation

we will only keep $M \neq 0$, and neglect m in the following, since m is smaller than M, m_ℓ or M_W . Inserting $\Gamma_{1b}^\mu(\ell)$ between $\bar{u}(p)$ and $u(P)$, making use of Dirac equations for these spinors and adopting the standard Feynman parameterization² for the denominator of (3):

$$\frac{1}{[(k-p)^2 - \xi M_W^2][(P-k)^2 - \xi M_W^2][k^2 - m_\ell^2]} = \int_0^1 dx \int_0^{1-x} \frac{2dy}{[k^2 - 2k \cdot (pz + Py) - (\xi M_W^2(1-x) + m_\ell^2 x)]^3}$$

with $z = 1 - x - y$. When we perform the d^4k integration of (3), the quadratic term in k of the numerator yields a logarithmic ultraviolet (UV) divergence. To handle this UV, we adopt² the 't Hooft–Veltman dimensional regularization by replacing the space-time 4 dimensions with $n + 2\epsilon$ ($4 \leftrightarrow n + 2\epsilon$), and the UV is symbolized by the singular Euler function $\Gamma(\epsilon) \approx 1/\epsilon$ for $\epsilon \rightarrow 0$. We will show that these $\Gamma(\epsilon)$ either mutually cancel out among the six diagrams, or identically vanish due to $\sum_\ell U_{L\ell} U_{H\ell}^* = 0$ reflecting the Glashow–Iliopoulos–Maiani (GIM) mechanism. The final result which must be finite is obtained by putting $\epsilon = 0$ at the end. The presence of γ_5 in n dimensions does not cause any ambiguity because we do not compute the traces of Dirac matrices in our $d^n k$ integration here. (About the problem of γ_5 in n dimensions, see for instance reference 2).

We get after the $d^n k$ integration of (3):

$$\Gamma_{1b}^\mu(\ell) = \frac{1}{8\pi^2} (1 + \gamma_5) \int_0^1 dx \int_0^{1-x} dy \frac{\mathcal{N}_b^\mu}{\mathcal{D}_1(\ell)}, \quad (4)$$

where

$$\mathcal{D}_1(\ell) = M_W^2 [\xi(1-x) + r_\ell x] - M^2 xy - q^2 y(1-x-y), \quad r_\ell = \frac{m_\ell^2}{M_W^2}, \quad (5)$$

$$\mathcal{N}_b^\mu = r_\ell \left\{ M(1-y)[(2y-1)P^\mu + (1-2x-2y)p^\mu] + \mathcal{D}_1(\ell) \left\{ \Gamma(\epsilon) - \log[\mathcal{D}_1(\ell)/M_W^2] \right\} \gamma^\mu \right\}. \quad (6)$$

Let us first discuss the question of UV divergences in the six amplitudes. As can be seen in (17) and (24), the divergences $\Gamma(\epsilon)$ of diagrams 1a and 2a are multiplied by ℓ -independent coefficients, respectively +6 and -2. Because of this fact, these UV become harmless when the three internal charged lepton contributions are summed up, due to the unitarity of \mathcal{U}_{lep} which tells us that $\sum_\ell U_{L\ell} U_{H\ell}^* \Gamma(\epsilon) = \Gamma(\epsilon) \sum_\ell U_{L\ell} U_{H\ell}^* = 0$. This is the essence of the GIM mechanism². On the other hand, as can be seen explicitly in (9), the coefficient r_ℓ of $\Gamma(\epsilon)$ in $\Gamma_{1b}^\mu(\ell)$ is ℓ -dependent, so $\sum_\ell U_{L\ell} U_{H\ell}^* r_\ell \Gamma(\epsilon) \neq 0$. This UV will be exactly canceled by that in Fig.2b, as given by (27). Finally, the amplitudes of diagrams 1c and 1d are ultraviolet convergent.

The $\log[\mathcal{D}_1(\ell)/M_W^2]$ term in (6) is the finite part extracted from

$$\mathcal{D}_1^{-\epsilon}(\ell) \Gamma(\epsilon) = [1 - \epsilon \log(\mathcal{D}_1(\ell)/M_W^2)] \Gamma(\epsilon) + \mathcal{O}(\epsilon).$$

The first term of \mathcal{N}_b^μ on the right hand side of (6) can be rewritten as

$$M(1-y)[-2xP^\mu + (2x+2y-1)q^\mu] . \quad (7)$$

By translational invariance, the neutrinos-photon vertex Γ^μ depends only on the four-momentum transfer q^μ and not on P^μ , the latter may be written as a combination of three independent vectors $i\sigma^{\mu\nu}q_\nu$, q^μ , and γ^μ by using the following relation valid for $m=0$,

$$2\bar{u}(p)(1+\gamma_5)P^\mu u(P) = \bar{u}(p)(1+\gamma_5)[i\sigma^{\mu\nu}q_\nu + M\gamma^\mu + q^\mu]u(P) . \quad (8)$$

Putting altogether (4)–(8), the ratio $\mathcal{N}_b^\mu/\mathcal{D}_1(\ell)$ in (4) can be rewritten as

$$\frac{\mathcal{N}_b^\mu}{\mathcal{D}_1(\ell)} = r_\ell \left\{ \frac{iM\sigma^{\mu\nu}q_\nu x(y-1)}{\mathcal{D}_1(\ell)} + \frac{q^\mu}{\mathcal{D}_1(\ell)}(y-1)(1-x-2y) + \frac{M^2\gamma^\mu}{\mathcal{D}_1(\ell)}x(y-1) + [\Gamma(\varepsilon) - \log[\mathcal{D}_1(\ell)/M_W^2]]\gamma^\mu \right\} . \quad (9)$$

For real photon emission $\nu_H \rightarrow \nu_L + \gamma$, only the $\sigma^{\mu\nu}q_\nu$ term in (9) contributes to the decay amplitude^{3,4}; this property is due to the conservation of the electromagnetic current, i.e. $\partial_\mu J_{em}^\mu = 0$. Indeed, the $\nu_H \rightarrow \nu_L + \gamma$ amplitude is written as $\langle \nu_L(p) | J_{em}^\mu | \nu_H(P) \rangle = \varepsilon_\mu^*(q)$ and the matrix element of the current J_{em}^μ has the most general Lorentz covariant form

$$\langle \nu_L(p) | J_{em}^\mu | \nu_H(P) \rangle = \bar{u}(p) \left[(a + b\gamma_5) i\sigma^{\mu\nu}q_\nu + (c + d\gamma_5)\gamma^\mu + (e + f\gamma_5)q^\mu \right] u(P) .$$

The condition $q_\mu \langle \nu_L(p) | J_{em}^\mu | \nu_H(P) \rangle = 0$ implies that only the magnetic form factors a, b survive, the c, d terms must vanish using the Dirac equation applied to $\bar{u}(p)$, $u(P)$, and finally the e, f terms proportional to q^μ do not contribute when multiplied by $\varepsilon_\mu^*(q)$.

Note that for the virtual photon case as in $\nu_H(P) \rightarrow \nu_L(p) + e^+(k_+) + e^-(k_-)$ of Fig.4, the $q^\mu = (k_- + k_+)^\mu$ term is also irrelevant because it vanishes when contracted with the conserved vector current $\bar{u}(k_-)\gamma_\mu v(k_+)$ of the electron-pair .

To obtain the $\nu_H \rightarrow \nu_L + \gamma$ decay amplitude \mathcal{A}_{1b} from Fig.1b according to (2)–(6), we perform the x, y integrations of the first term $[x(y-1)/\mathcal{D}_1(\ell)] iM\sigma^{\mu\nu}q_\nu$ in (9). For that, we will neglect $M^2xy \ll M_W^2$ in $\mathcal{D}_1(\ell)$ to simplify the computation, and put $q^2 = 0$ since we are dealing with a real photon. Thus (2) becomes:

$$\mathcal{A}_{1b} = \mathcal{A}_0 \sum_\ell U_{H\ell} U_{L\ell}^* F_{1b}(\ell) , \quad (10)$$

where

$$\mathcal{A}_0 = \frac{G_F}{\sqrt{2}} \frac{e}{8\pi^2} \bar{u}(p) [M(1+\gamma_5)] i\sigma^{\mu\nu}q_\nu u(P) \varepsilon_\mu^*(q) \quad (11)$$

$$F_{1b}(\ell) = \frac{\xi r_\ell^2 (r_\ell - 2\xi) \log(r_\ell/\xi)}{2(r_\ell - \xi)^4} + r_\ell \left[-\frac{1}{3(r_\ell - \xi)} - \frac{\xi}{4(r_\ell - \xi)^2} + \frac{\xi^2}{2(r_\ell - \xi)^3} \right] , \quad (12)$$

with the Fermi constant $G_F = g^2/(4\sqrt{2}M_W^2)$. If m is not neglected, the $[M(1+\gamma_5)]$ term in (11) would be replaced by $[M(1+\gamma_5) + m(1-\gamma_5)]$. If we keep M^2xy in $\mathcal{D}_1(\ell)$, we still obtain an explicit analytic form for $F_{1b}(\ell)$; the result is complicated and not illuminating however. The exact formula (12) is in agreement with similar calculations³ for $\mu^- \rightarrow e^- + \gamma$ in the limit $r_\ell \rightarrow 0$, where only the linear term in r_ℓ was kept and the logarithmic term neglected. In the same reference 3, the ξ -dependences of the four diagrams similar to Fig.1a–d are explicitly shown to mutually canceled out, leaving the final result ξ -independent. In the following, we will compute the five other amplitudes in the Feynman–t Hooft gauge ($\xi = 1$), for which (12) becomes

$$F_{1b}(\ell) = \frac{r_\ell^2(r_\ell - 2) \log r_\ell}{2(r_\ell - 1)^4} + r_\ell \left[-\frac{1}{3(r_\ell - 1)} - \frac{1}{4(r_\ell - 1)^2} + \frac{1}{2(r_\ell - 1)^3} \right]. \quad (13)$$

The singularities of $F_{1b}(\ell)$ at $r_\ell = 1$ are only apparent, in fact $F_{1b}(\ell) = -1/8$ for $r_\ell = 1$.

- By the same method just outlined, the \mathcal{A}_{1a} amplitude of Fig.1a in the $\xi = 1$ gauge is given by

$$i \mathcal{A}_{1a} = (ie) \left(\frac{-ig}{2\sqrt{2}} \right)^2 \sum_\ell U_{L\ell} U_{H\ell}^* \bar{u}(p) \Gamma_{1a}^\mu(\ell) u(P) \varepsilon_\mu^*(q) \quad (14)$$

$$\begin{aligned} \Gamma_{1a}^\mu(\ell) &= \int \frac{d^4k}{(2\pi)^4} \frac{\gamma_\rho(1-\gamma_5)[i(\not{k} + m_\ell)]\gamma_\sigma(1-\gamma_5)X^{\mu\rho\sigma}}{[(k-p)^2 - M_W^2][(P-k)^2 - M_W^2](k^2 - m_\ell^2)} \\ X^{\mu\rho\sigma} &= (k+p-2P)^\rho g^{\mu\sigma} + (k+P-2p)^\sigma g^{\rho\mu} + (P+p-2k)^\mu g^{\rho\sigma}. \end{aligned} \quad (15)$$

We get

$$\Gamma_{1a}^\mu = \frac{1}{8\pi^2}(1+\gamma_5) \int_0^1 dx \int_0^{1-x} dy \frac{\mathcal{N}_{1a}^\mu}{\mathcal{D}_1(\xi=1, x)} \quad (16)$$

$$\begin{aligned} \mathcal{N}_{1a}^\mu &= \left\{ [2(1-x)(1-y) + y]M^2 - 2[(1-x)(1-y) + y^2]q^2 + 6\mathcal{D}_1^{1-\epsilon}(\ell)\Gamma(\epsilon) \right\} \gamma^\mu \\ &\quad + 2M \left\{ y(1-2y)P^\mu + [2y^2 - (1-x)(1+2y)]p^\mu \right\} \end{aligned} \quad (17)$$

The first term of \mathcal{N}_{1a}^μ proportional to γ^μ does not contribute to the real photon process $\nu_H \rightarrow \nu_L + \gamma$.

The second term, coefficient of $2M$, may be rewritten as

$$y(1-2y)P^\mu + [2y^2 - (1-x)(1+2y)]p^\mu = [y - (1-x)(1+2y)]P^\mu + Cq^\mu,$$

and as before the P^μ term is converted into form (8). We get for (16)

$$\begin{aligned} \frac{\mathcal{N}_{1a}^\mu}{\mathcal{D}_1(\ell)} &= \frac{iM\sigma^{\mu\nu}q_\nu}{\mathcal{D}_1(\ell)}[x-1-y(1-2x)] + \frac{\not{q}q^\mu}{\mathcal{D}_1(\ell)}[1-x+3y-2xy-4y^2] \\ &\quad + \frac{M^2\gamma^\mu}{\mathcal{D}_1(\ell)}[1-x-2y(1-2x)] - \frac{2q^2\gamma^\mu}{\mathcal{D}_1(\ell)}[y^2 + (1-x)(1-y)] + 6\left\{ \Gamma(\epsilon) - \log[\mathcal{D}_1(\ell)/M_W^2] \right\} \gamma^\mu. \end{aligned} \quad (18)$$

After the x, y integrations of the first term in (18) relevant for the real photon case, we obtain the contribution from Fig.1a written in the form (10)–(12) with $F_{1b}(\ell)$ replaced by $F_{1a}(\ell)$, the latter is given by

$$F_{1a}(\ell) = \frac{r_\ell^2(1-3r_\ell)\log r_\ell}{2(r_\ell-1)^4} + r_\ell \left[\frac{7}{12(r_\ell-1)} + \frac{2}{(r_\ell-1)^2} + \frac{1}{(r_\ell-1)^3} \right] - \frac{7}{12} \quad (19)$$

The singularities of $F_{1a}(\ell)$ at $r_\ell = 1$ are only apparent, actually $F_{1a}(\ell)$ is equal to $-5/12$ for $r_\ell = 1$.

The remaining amplitudes derived from the diagrams of Fig.1c,d and Fig.2a,b are given below:

- Fig.1c :
$$\frac{\mathcal{N}_{1c}^\mu}{\mathcal{D}_1(\ell)} = \frac{iM\sigma^{\mu\nu}q_\nu}{\mathcal{D}_1(\ell)}(x+y-1) + \frac{\not{q}q^\mu}{\mathcal{D}_1(\ell)}(1-x-y) + \frac{M^2\gamma^\mu}{\mathcal{D}_1(\ell)}(x-1) + \frac{m_\ell^2\gamma^\mu}{\mathcal{D}_1(\ell)}, \quad (20)$$

which gives after the x, y integrations

$$F_{1c}(\ell) = \frac{-r_\ell^2\log r_\ell}{2(r_\ell-1)^3} + r_\ell \left[\frac{1}{4(r_\ell-1)} + \frac{1}{2(r_\ell-1)^2} \right] - \frac{1}{4}. \quad (21)$$

- Fig.1d :
$$\frac{\mathcal{N}_{1d}^\mu}{\mathcal{D}_1(\ell)} = \frac{m_\ell^2\gamma^\mu}{\mathcal{D}_1(\ell)}, \quad (22)$$

thus

$$F_{1d}(\ell) = 0. \quad (23)$$

- Fig.2a :
$$\begin{aligned} \frac{\mathcal{N}_{2a}^\mu}{\mathcal{D}_2(\ell)} &= \frac{2iM\sigma^{\mu\nu}q_\nu}{\mathcal{D}_2(\ell)}x(y-1) + \frac{2\not{q}q^\mu}{\mathcal{D}_2(\ell)}(1-y)(x+2y) - \frac{2m_\ell^2\gamma^\mu}{\mathcal{D}_2(\ell)} \\ &+ \frac{2q^2\gamma^\mu}{\mathcal{D}_2(\ell)}(y-1)(x+y) - 2\left\{\Gamma(\varepsilon) - \log[\mathcal{D}_2(\ell)/M_W^2]\right\}\gamma^\mu, \end{aligned} \quad (24)$$

where

$$\mathcal{D}_2(\ell) = M_W^2x + m_\ell^2(1-x) - M^2xy - q^2y(1-x-y). \quad (25)$$

We get

$$F_{2a}(\ell) = \frac{r_\ell(2r_\ell-1)\log r_\ell}{(r_\ell-1)^4} + r_\ell \left[\frac{2}{3(r_\ell-1)} - \frac{3}{2(r_\ell-1)^2} - \frac{1}{(r_\ell-1)^3} \right] - \frac{2}{3}. \quad (26)$$

Finally,

- Fig.2b :
$$\begin{aligned} \frac{\mathcal{N}_{2b}^\mu}{\mathcal{D}_2(\ell)} &= r_\ell \left\{ \frac{iM\sigma^{\mu\nu}q_\nu}{\mathcal{D}_2(\ell)}[x(1+y)-1] + \frac{\not{q}q^\mu}{\mathcal{D}_2(\ell)}[1-x(1+y)-2y^2] - \frac{m_\ell^2\gamma^\mu}{\mathcal{D}_2(\ell)} \right. \\ &+ \left. \frac{M^2\gamma^\mu}{\mathcal{D}_2(\ell)}x + \frac{q^2\gamma^\mu}{\mathcal{D}_2(\ell)}y(x+y-1) - \left\{ \Gamma(\varepsilon) - \log[\mathcal{D}_2(\ell)/M_W^2] \right\} \gamma^\mu \right\}, \end{aligned} \quad (27)$$

from which

$$F_{2b}(\ell) = \frac{r_\ell(2-r_\ell)\log r_\ell}{2(r_\ell-1)^4} + r_\ell \left[\frac{-5}{12(r_\ell-1)} + \frac{3}{4(r_\ell-1)^2} - \frac{1}{2(r_\ell-1)^3} \right]. \quad (28)$$

The constants $(-7/12), (-1/4), (-2/3)$ respectively in (19), (21) and (26) being ℓ -independent do not contribute to the decay amplitude when summed over ℓ , due to $\sum_{\ell} U_{H\ell}^* U_{L\ell} = 0$. The sum of the six terms $\sum_{\ell} U_{H\ell} U_{L\ell}^* [F_{1,a\dots d}(\ell) + F_{2,a,b}(\ell)]$ yields the final result for the $\nu_H \rightarrow \nu_L + \gamma$ decay amplitude

$$\mathcal{A}(\nu_H \rightarrow \nu_L + \gamma) = \frac{3\mathcal{A}_0}{4} \sum_{\ell} \frac{U_{H\ell} U_{L\ell}^* r_{\ell}}{(1 - r_{\ell})^3} \left[1 - r_{\ell}^2 + 2r_{\ell} \log r_{\ell} \right], \quad (29)$$

where \mathcal{A}_0 is defined in (11). Our result (29) agrees with formula (10.28) for the function $f(r)$ in reference 4, where the three irrelevant constants mentioned above are kept. We get

$$\Gamma_0 \equiv \Gamma(\nu_H \rightarrow \nu_L + \gamma) = \frac{G_F^2 M^5}{192\pi^3} \left(\frac{27\alpha}{32\pi} \right) \left| \sum_{\ell} \frac{U_{H\ell} U_{L\ell}^* r_{\ell}}{(1 - r_{\ell})^3} \left[1 - r_{\ell}^2 + 2r_{\ell} \log r_{\ell} \right] \right|^2. \quad (30)$$

We assume for \mathcal{U}_{lep} the following form⁵ :

$$\mathcal{U}_{\text{lep}} = \begin{pmatrix} \cos \theta_{12} & -\sin \theta_{12} & 0 \\ \frac{1}{\sqrt{2}} \sin \theta_{12} & \frac{1}{\sqrt{2}} \cos \theta_{12} & \frac{-1}{\sqrt{2}} \\ \frac{1}{\sqrt{2}} \sin \theta_{12} & \frac{1}{\sqrt{2}} \cos \theta_{12} & \frac{1}{\sqrt{2}} \end{pmatrix}. \quad (31)$$

The mixing angle $\theta_{23} \approx 45^0$ is suggested by the Super-Kamiokande data and the $\theta_{13} \approx 0^0$ comes from the Chooz data^{1,5} which give $\theta_{13} \leq 13^0$, whereas θ_{12} is arbitrary. Although θ_{12} is likely small $\approx 0^0$, the maximal mixing $\theta_{12} \approx 45^0$ could be possible which would allow $\nu_e \leftrightarrow \nu_{\mu}$ oscillations (as suggested by the LSND experiment^{1,5}). Taking θ_{12} in the range 0^0 – 45^0 , and $M = 5 \times 10^{-2}$ eV, the decay rate $\Gamma(\nu_H \rightarrow \nu_L + \gamma)$ is found to be $\approx 10^{-44}$ /year.

2- The mode $\nu_H \rightarrow \nu_L + e^+ + e^-$

If kinematically allowed, i.e. if the mass difference $M-m$ between the two neutrinos is larger than twice the electron mass, the decay $\nu_H(P) \rightarrow \nu_L(p) + e^+(k_+) + e^-(k_-)$ is possible, and governed by the tree diagram in Fig.3. The corresponding amplitude is

$$\mathcal{A}_{\text{tree}} = \frac{G_F}{\sqrt{2}} U_{He}^* U_{Le} \bar{u}(k_-) \gamma^{\mu} (1 - \gamma_5) u(P) \bar{u}(p) \gamma_{\mu} (1 - \gamma_5) v(k_+). \quad (32)$$

Using Fierz recombination² and $U_{He}^* U_{Le} = -\sum_{\ell'=\mu,\tau} U_{H\ell'}^* U_{L\ell'}$, this amplitude can be rewritten as

$$\mathcal{A}_{\text{tree}} = (-1)^2 \frac{G_F}{\sqrt{2}} \sum_{\ell'=\mu,\tau} U_{H\ell'}^* U_{L\ell'} \bar{u}(p) \gamma^{\mu} (1 - \gamma_5) u(P) \bar{u}(k_-) \gamma_{\mu} (1 - \gamma_5) v(k_+). \quad (33)$$

Electromagnetic radiative corrections to $\mathcal{A}_{\text{tree}}$ come from the six diagrams previously considered; the emitted photon is now virtual and creates an electron pair (Fig.4).

A careful examination of all the terms in (9), (18), (20), (22), (24) and (27) of the six vertices $\Gamma_{1a-d}^{\mu}(\ell), \Gamma_{2a,b}^{\mu}(\ell)$ shows that after the x, y integrations, the largely dominant contribution comes from

Fig.2a with the q^2 term in (24) which exhibits an infrared-like divergence $\log r_\ell \rightarrow \infty$ for $r_\ell \rightarrow 0$. We can track down this divergent behavior by examining the integration limits $x = 0$ and $x = 1$ of the denominators $\mathcal{D}_{1,2}(\ell)$. Infrared-like divergence occurs if the numerators $\mathcal{N}_2^\mu(\ell)$ lack an x term to cancel the $x = 0$ integration limit of the $x M_W^2$ term in the denominator $\mathcal{D}_2(\ell)$ in (25). This happens with the $2y(1-y)q^2$ term of $\mathcal{N}_{2a}^\mu(\ell)$ in (24) which cannot cancel the $x M_W^2$ in $\mathcal{D}_2(\ell)$ and gives the dominant $\log r_\ell$ behavior, reflecting mass singularities (or infrared divergences) of loop integrals. Except this $\log r_\ell$, *all other terms* of the six vertices are negligibly small because they are strongly damped by powers of r_ℓ , or $r_\ell^n \log r_\ell$ where $n > 0, r_\ell < 10^{-3}$. Indeed, the four diagrams of Fig.1 are strongly damped since infrared-like divergence cannot occur: the $x = 1$ integration limit of the $(1-x)M_W^2$ in the denominator $\mathcal{D}_1(\ell)$ is systematically canceled by the $1-x$ coming from the integration over the y variable. Also Fig.2b is damped by $r_\ell \log r_\ell$, due to the Φ -fermions coupling.

Explicit x, y integrations of all the six vertices $\Gamma_{1a-d}^\mu(\ell), \Gamma_{2a,b}^\mu(\ell)$ confirm these features. The $\log r_\ell$ infrared-like divergence, which arises when there are two massless ($r_\ell = 0$) fermion propagators in the loop, has been noticed a long time ago in the neutrino charge radius computations⁶.

This leading $q^2 \log r_\ell$ term of Fig.2a in the $\nu_H - \nu_L - \gamma^*$ vertex cancels the photon propagator $1/q^2$ in Fig.4 and yields an effective local four-fermion coupling proportional to G_F . Thus the radiative correction to the $\nu_H \rightarrow \nu_L + e^+ + e^-$ tree amplitude is found to be

$$\mathcal{A}_{rad} = \frac{G_F}{\sqrt{2}} \frac{e^2}{24\pi^2} \left[\sum_\ell U_{H\ell}^* U_{L\ell} \log r_\ell \right] \bar{u}(p) \gamma^\mu (1 - \gamma_5) u(P) \bar{u}(k_-) \gamma_\mu v(k_+) , \quad (34)$$

which can be put in a form similar to \mathcal{A}_{tree} in (33):

$$\mathcal{A}_{rad} = \frac{G_F}{\sqrt{2}} \frac{e^2}{24\pi^2} \left[\sum_{\ell'=\mu,\tau} U_{H\ell'}^* U_{L\ell'} \log \frac{m_{\ell'}^2}{m_e^2} \right] \bar{u}(p) \gamma^\mu (1 - \gamma_5) u(P) \bar{u}(k_-) \gamma_\mu v(k_+) . \quad (35)$$

The sum $\mathcal{A}_{tree} + \mathcal{A}_{rad} \equiv \mathcal{B}$ is now easy to manipulate when we take the interference between \mathcal{A}_{tree} and \mathcal{A}_{rad} in $|\mathcal{B}|^2$ for the decay rate. Thus

$$\mathcal{B} = \frac{G_F}{\sqrt{2}} \bar{u}(p) \gamma^\mu (1 - \gamma_5) u(P) \bar{u}(k_-) \gamma_\mu (g_V - g_A \gamma_5) v(k_+) , \quad (36)$$

with

$$g_V = \sum_{\ell'=\mu,\tau} U_{H\ell'}^* U_{L\ell'} \left(1 + \frac{\alpha}{3\pi} \log \frac{m_{\ell'}}{m_e} \right) , \quad g_A = \sum_{\ell'=\mu,\tau} U_{H\ell'}^* U_{L\ell'} . \quad (37)$$

From the amplitude \mathcal{B} , we compute⁷ the decay rate $\Gamma_1 \equiv \Gamma(\nu_H \rightarrow \nu_L + e^+ + e^-)$ and find

$$\frac{d\Gamma_1}{dq^2} = \frac{G_F^2}{192\pi^3} \frac{\sqrt{q^2(q^2 - 4m_e^2)}}{q^4 M^3} (M^2 - q^2)^2 \left\{ (g_V^2 + g_A^2) [q^2(M^2 + 2q^2) + 2m_e^2(M^2 - q^2)] + 6m_e^2 q^2 (g_V^2 - g_A^2) \right\} , \quad (38)$$

from which we get

$$\Gamma_1 = \int_{4m_e^2}^{M^2} dq^2 \frac{d\Gamma_1}{dq^2} = \frac{G_F^2 M^5}{192\pi^3} \left\{ \frac{g_V^2 + g_A^2}{2} G(x) + (g_V^2 - g_A^2) H(x) \right\}, \quad (39)$$

where $x = m_e^2/M^2$, and $G(x), H(x)$ are the phase-space functions given by

$$G(x) = \left[1 - 14x - 2x^2 - 12x^3 \right] \sqrt{1-4x} + 24x^2(1-x^2) \log \frac{1 + \sqrt{1-4x}}{1 - \sqrt{1-4x}}, \quad (40)$$

$$H(x) = 2x(1-x)(1+6x)\sqrt{1-4x} + 12x^2(2x-1-2x^2) \log \frac{1 + \sqrt{1-4x}}{1 - \sqrt{1-4x}}. \quad (41)$$

To this leading logarithm radiative correction expressed by $\approx \alpha \log r$ in (37)-(39), we may also add the nonleading (simple α without $\log r$) electromagnetic correction to the e^+e^- pair. This nonleading QED correction can be obtained from the one-loop QCD correction to the well known $e^+e^- \rightarrow$ quark-pair cross-section, or the $\tau \rightarrow \nu_\tau +$ quark-pair decay rate which is already computed in the literature². The only appropriate change is the substitution $(4/3)\alpha_s \leftrightarrow \alpha$, because when going from QCD to QED, we replace a gluon with a photon and the quark-pair with the electron-pair, the QCD vertex $ig_s\gamma^\mu\lambda_j/2$ is replaced with the QED vertex $ie\gamma^\mu$ and the factor $4/3$ comes from $4/3 = (1/4)\sum_j \lambda_j\lambda_j$, where λ_j are the eight Gell-Mann matrices of the color $SU_c(3)$ group.

This QED nonleading corrected rate Γ_2 is

$$\Gamma_2 = \frac{G_F^2 M^5}{192\pi^3} \left(\frac{3\alpha}{4\pi} \right) G(x) K(x, x); \quad (42)$$

the function $K(x, x)$ is tabulated in Table 14.1 of reference 2. We emphasize that $K(x, x)$ is a spectacular increasing function of x , acting in opposite direction to the decreasing phase-space function $G(x)$. As announced, the $\nu_H \rightarrow \nu_L + e^+ + e^-$ decay rate given by the sum $\Gamma_1 + \Gamma_2$ in (39)–(42) largely dominates the $\nu_H \rightarrow \nu_L + \gamma$ in (30). Finally we note that the virtual weak neutral Z boson replacing the virtual photon in Fig.4 also contributes to $\nu_H \rightarrow \nu_L + e^+ + e^-$. However it can be safely discarded, being strongly damped by q^2/M_Z^2 due to the Z propagator.

Conclusions

The recent observation by the Super-Kamiokande collaboration of a clear up-down ν_μ asymmetry in atmospheric neutrinos is strongly suggestive of $\nu_\mu \rightarrow \nu_X$ oscillations, where ν_X may be identified with ν_τ or even possibly a sterile neutrino. These results have many important implications in elementary particle physics and astrophysics⁸. In particular, neutrino oscillations mean that neutrinos have a non-vanishing mass, which, according to the new data, may be at least as heavy as 5×10^{-2} eV. If a neutrino ν_H has indeed a mass, it may not be stable and could decay into a lighter neutrino, ν_L , through a cross-family electroweak coupling. We have studied two such decay modes, $\nu_H \rightarrow \nu_L + \gamma$ and

$\nu_H \rightarrow \nu_L + e^+ + e^-$, and found that the latter, which, in contrast to the former, arises at the tree level and gets largely enhanced by radiative corrections, is by far the dominant process and may therefore be detectable provided that ν_H has a mass $> 2 m_e$. A positive evidence for such decay modes would give a clear signal of the onset of ‘new physics’.

References

- [1] Janet Conrad and M. Takita, Talks at the XXIX International Conference on High Energy Physics, Vancouver, Canada July 1998
Y. Fukuda et al., Phys. Rev. Lett. **81**, 1562 (1998)
- [2] The calculational method of loop integrals is explained in many textbooks, see for instance Q. Ho-Kim and X.Y. Pham, *Elementary Particles and their Interactions. Concepts and Phenomena*, chapter 14 and appendix A3. Springer, Berlin, Heidelberg 1998
- [3] T.P. Cheng and L.F. Li, *Gauge Theory of Elementary Particle Physics*, page 426. Oxford University Press, New York 1984
- [4] R.N. Mohapatra and P.B. Pal, *Massive Neutrinos in Physics and Astrophysics*, page 183. World Scientific, Singapore 1991
- [5] R.D. Peccei, Summary talk at the XXIX International Conference on High Energy Physics, Vancouver, Canada July 1998
- [6] J. Bernstein and T.D. Lee, Phys. Rev. Lett. **11**, 512 (1963)
C. Bouchiat, J. Iliopoulos and Ph. Meyer, Phys. Lett. **42B**, 91 (1972)
- [7] The calculation of the $F \rightarrow f_1 + f_2 + \bar{f}_3$ decay rate is explained for instance in ref. 2, chapter 13, where F, f_i stand for fermions
- [8] A. de Rujula and S. Glashow, Phys. Rev. Lett. **45**, 942 (1980).

EXERCISES 1- Show that the ξ -dependences of Fig.2a and Fig.2b amplitudes exactly cancel out, leaving their sum ξ -independent.

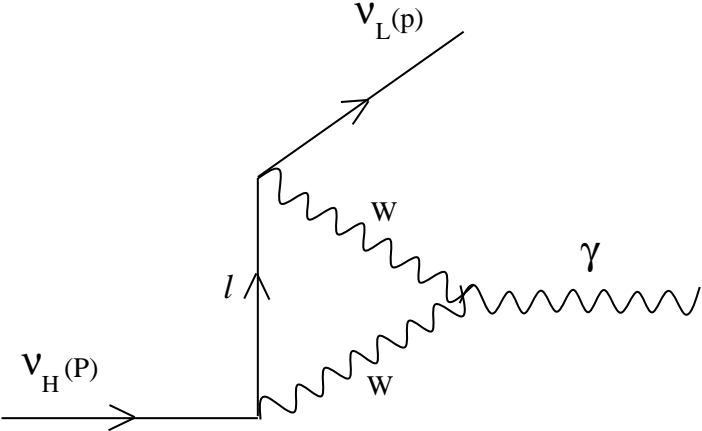
2- Explain qualitatively why the lifetimes jump from 10^{-2} year to 10^{44} years when the neutrino mass changes from 1.1 MeV to 5×10^{-2} eV.

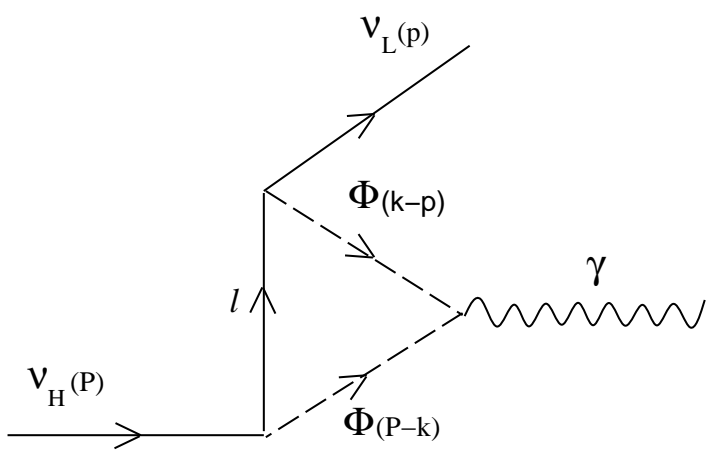
Figure Captions :

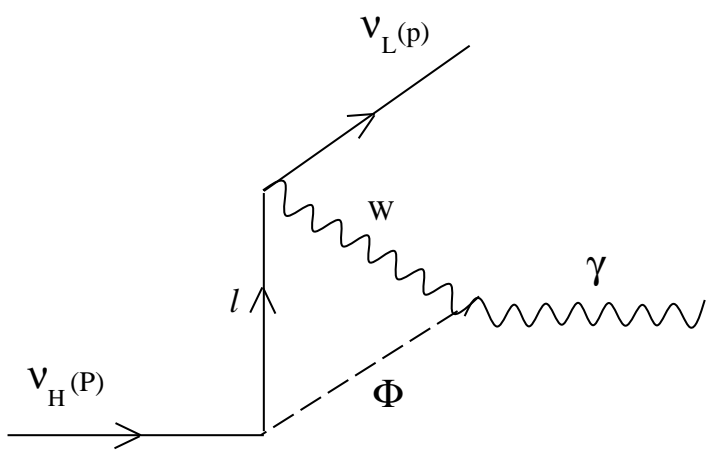
Figures 1–2 : One-loop $\nu_H \rightarrow \nu_L + \gamma$ in the renormalizable R_ξ -gauge.

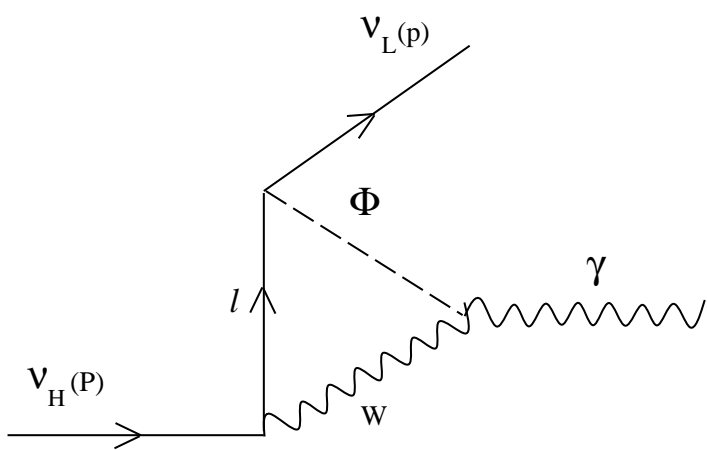
Figure 3 : Tree diagram $\nu_H \rightarrow \nu_L + e^+ + e^-$

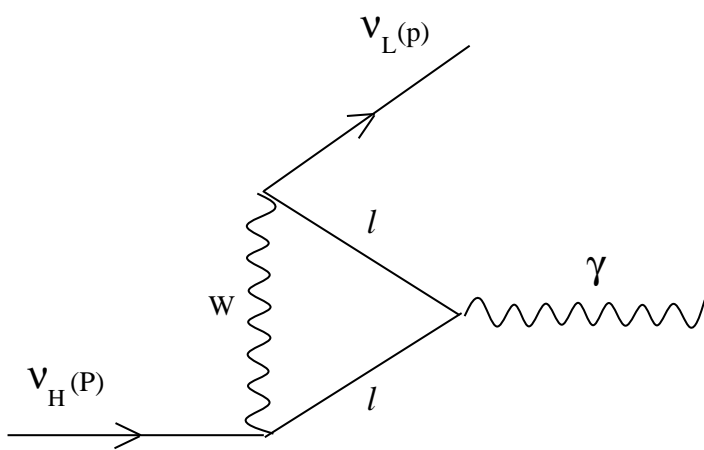
Figure 4 : Leading radiative corrections to $\nu_H \rightarrow \nu_L + e^+ + e^-$

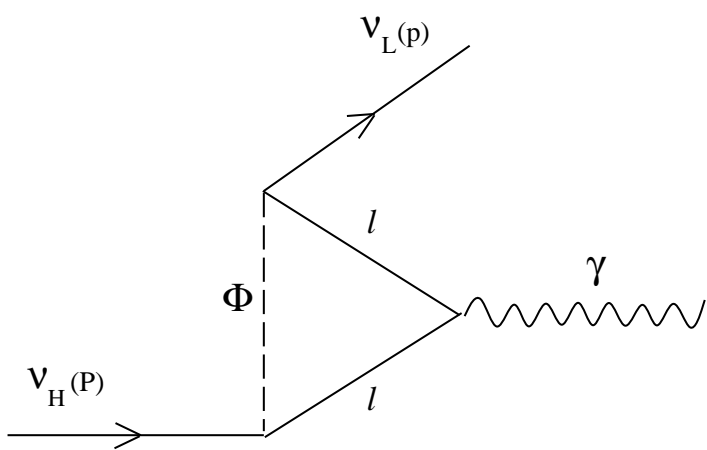


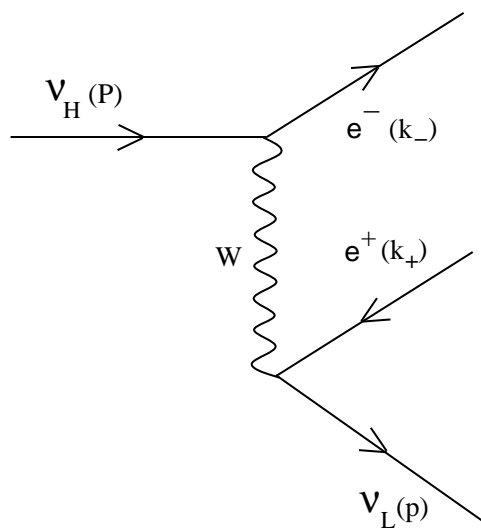


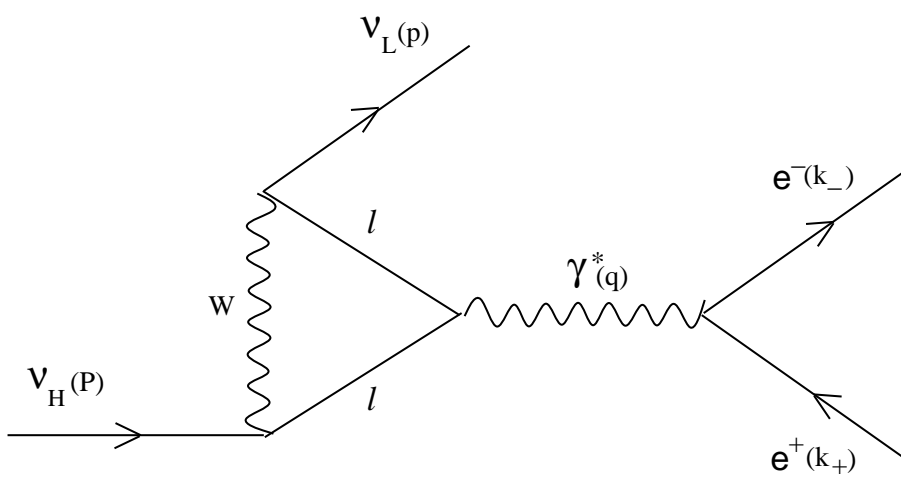








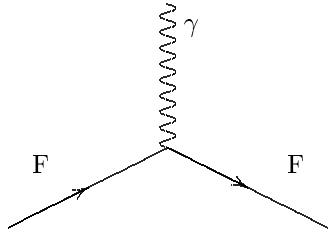




APPENDIX

FEYNMAN RULES: Some VERTICES and PROPAGATORS in the R_ξ GAUGE

VERTICES in general

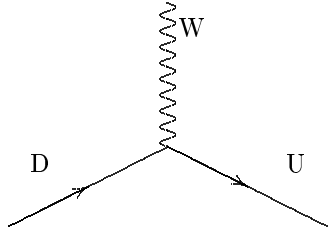


$$-i e Q \gamma_\mu \quad (e > 0)$$

$$Q = -1 \text{ for } F = \ell^- (e^-, \mu^-, \tau^-)$$

$$Q = \frac{2}{3} \text{ for } F = U \text{ (u, c, t) quarks}$$

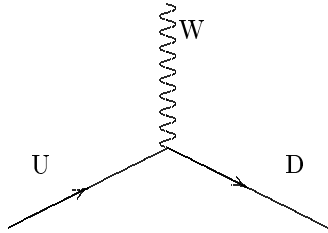
$$Q = -\frac{1}{3} \text{ for } F = D \text{ (d, s, b) quarks}$$



$$-i g \frac{1}{2\sqrt{2}} \gamma_\mu (1 - \gamma_5) V_{UD}$$

$$U \equiv (u, c, t) \text{ quarks, or } \nu_i \text{ massive neutrinos}$$

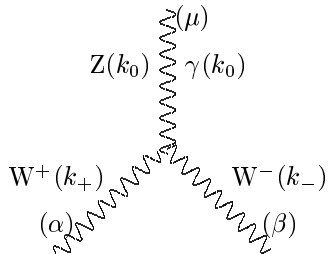
$$D \equiv (d, s, b) \text{ quarks, or } e^-, \mu^-, \tau^- \text{ leptons}$$



$$-i g \frac{1}{2\sqrt{2}} \gamma_\mu (1 - \gamma_5) V_{UD}^*$$

$$U \equiv (u, c, t) \text{ quarks, or } \nu_i \text{ massive neutrinos}$$

$$D \equiv (d, s, b) \text{ quarks, or } e^-, \mu^-, \tau^- \text{ leptons}$$

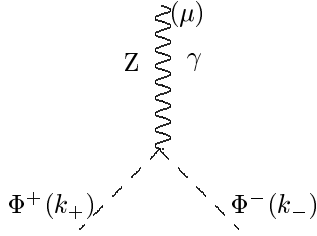


$$k_0 + k_+ + k_- = 0$$

$$\gamma WW \text{ vertex : } +ie [(k_+ - k_-)_\mu g_{\alpha\beta} + (k_- - k_0)_\alpha g_{\mu\beta} + (k_0 - k_+)_\beta g_{\mu\alpha}]$$

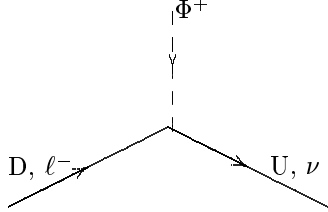
$$ZWW \text{ vertex : } +ig \cos \theta_W [(k_+ - k_-)_\mu g_{\alpha\beta} + (k_- - k_0)_\alpha g_{\mu\beta} + (k_0 - k_+)_\beta g_{\mu\alpha}]$$

VERTICES in R_ξ gauge

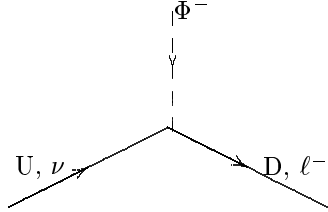


$$\gamma\Phi\Phi \text{ vertex: } -ie(k_+ - k_-)_\mu$$

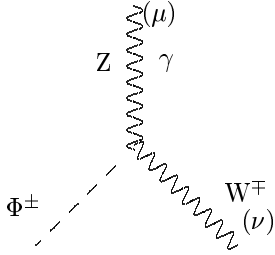
$$Z\Phi\Phi \text{ vertex: } -i g \frac{\cos 2\theta_W}{2 \cos \theta_W} (k_+ - k_-)_\mu$$



$$ig \frac{1}{2\sqrt{2}M_W} [m_U(1 - \gamma_5) - m_D(1 + \gamma_5)] V_{UD}$$



$$ig \frac{1}{2\sqrt{2}M_W} [m_U(1 + \gamma_5) - m_D(1 - \gamma_5)] V_{UD}^*$$



$$W\gamma\Phi \text{ vertex: } +ieM_W g_{\mu\nu}$$

$$ZW\Phi \text{ vertex: } -ig \frac{\sin^2 \theta_W}{\cos \theta_W} M_W g_{\mu\nu}$$

PROPAGATORS

$$\text{W boson : } \frac{i}{k^2 - M_W^2 + i\epsilon} \left[-g_{\mu\nu} + \frac{(1-\xi)k_\mu k_\nu}{k^2 - \xi M_W^2} \right] \xrightarrow{k \rightarrow \infty} \frac{i}{k^2}$$

$$\text{Goldstone boson } \Phi_W, \text{ associated with the W boson : } \frac{i}{k^2 - \xi M_W^2 + i\epsilon}$$

The Unitarity U gauge corresponds to $\xi = \infty$, for which only the physical W boson intervenes with the propagator

$$\frac{i}{k^2 - M_W^2 + i\epsilon} \left[-g_{\mu\nu} + \frac{k_\mu k_\nu}{M_W^2} \right] \xrightarrow{k \rightarrow \infty} \frac{i}{M_W^2}$$